Journal of Applied Polymer Science

Poly(ethylene oxide)-g-gellan polysaccharide nanocarriers for controlled gastrointestinal delivery of simvastatin

Sayantan Sadhukhan, Paromita Bakshi, Rana Datta, Sabyasachi Maiti
Department of Pharmaceutics, Gupta College of Technological Sciences, Ashram More, G.T Road, Asansol-713301 West Bengal, India
Correspondence to: S. Maiti (E-mail: sabya245@rediffmail.com)

ABSTRACT: Herein, a novel gellan polysaccharide-based amphiphilic copolymer was synthesized for the development of simvastatin-loaded micellar nanoparticles. The nanoparticles were explored for their controlled drug release and improved pharmacodynamic potentials. The copolymer was characterized by Fourier transform infrared spectroscopy (FTIR) and elemental analysis. The onset of copolymer micellization was detected by fluorescence spectroscopy. Simvastatin was loaded into micellar particles by solvent evaporation method and the particles were then characterized by microscopic and light scattering techniques. The physical state of drug was studied by X-ray diffraction analysis. Pharmacodynamic assessment of the micellar preparations was done on rabbit models. The copolymer formed micellar nanoparticles in water. Critical micellar concentration was 9.12mg/l. The micellar particles (426.8–912.6nm) entrapped a maximum of 18.86% drug. Higher negative zeta potential indicated physical stability of micellar systems. A simple diffusion mechanism was operative in the event of comparatively faster drug release in pH6.8 phosphate buffer solution. No significant drug-copolymer interaction was traced by FTIR spectroscopy. The amorphization of drug into micellar particles reduced LDL-cholesterol level by ~45% in hyperlipidemic rabbits and this was about 2.5 times higher than pure drug dispersion. Copolymer micellar nanoparticles of simvastatin could control cholesterol level in hyperlipidemic rabbits and thus had potential in drug delivery applications. © 2015 Wiley Periodicals, Inc. J. Appl. Polym. Sci. **2015**, *132*, 42399.

KEYWORDS: drug delivery systems; hydrophilic polymers; nanostructured polymers

Received 28 December 2014; accepted 21 April 2015
DOI: 10.1002/app.42399

INTRODUCTION

Natural polysaccharides are currently being investigated for the design of various pharmaceutical dosage forms because of their biodegradability and lack of oral toxicity. Gellan gum is water soluble polysaccharide and is composed of α-L-rhamnose, β-D-glucuronic acid and β-D-glucose residues (molar ratio 1 : 1 : 2) to form a linear primary structure.[1] It was approved for food use by the US Food and Drug Administration in 1992.[2] This report on safety gave an impetus to the development of gellan polysaccharide-based drug delivery devices such as ophthalmic gels,[3,4] hydrogel beads,[5,6] *in situ*-forming gels,[7–11] and matrix tablets for oral delivery.[12,13]

However, the reports on gellan polysaccharide-based nanoparticles for oral delivery are rare in the literature. Numbers of methods have been used for the preparation of synthetic polymer-based nanoparticles including emulsification/solvent evaporation, solvent displacement, emulsification/solvent diffusion, and interfacial deposition[14] however; the methods of production for polysaccharide-based nanoparticles are very limited. Ionotropic gelation of charged polysaccharides often led to coagulation/aggregation of polysaccharide sol due to uncontrolled addition of metallic salt solution. Even when the addition of metal ions was controlled, the polysaccharide pre-gel nucleus required further stabilization by oppositely charged polyelectrolytes in order to maintain individuality of the nanoparticles.[15,16] In recent years, nanoparticles in the form of micelles have emerged as new vehicles for oral delivery of poorly water soluble drugs.

Micellar drug carriers could provide a set of advantages: (a) physical entrapment of poorly soluble drugs and enhancement of their retention and bioavailability by preventing contact with enzymatic and acidic environment of gastrointestinal tract (GIT)[17–19] and (b) easy, reproducible production in large quantities.[20]

In addition, the hydrophilic shell could maintain physical stability of the micelles by keeping them in a dispersed state. Surfactant micelles tend to disintegrate upon dilution, and trigger the lysis of cell membranes;[21] whereas polymeric micelles by virtue

of their lower critical association concentration (CAC) are stable toward dilution and therefore, exhibit minimal cytotoxicity.[22,23]

In case of poorly water-soluble drugs, their dissolution rate is quite often the rate-limiting step for absorption from the gastrointestinal tract.[24] Sometimes, the dissolution times are longer than transit times to the intended absorptive sites.[25] Thus, the effective delivery of poorly water-soluble therapeutics was difficult *via* the oral route.[26]

On the basis of poor water solubility, about 40% of potential drugs identified through high throughput screening are rejected from formulation development.[27] Under such circumstances, the combined hydrophobic/hydrophilic structure of micelles could be beneficial. Despite these advantages, polysaccharide-based micellar systems are still under development and the outcomes have not met yet the clinical need.

Notable examples of polysaccharide-based micellar systems include dextran-*g*-PEO-C_{16},[28,29] methoxy poly (ethylene glycol)-*g*-chitosan,[30] and pullulan-*g*-poly (L-lactide),[31] cholesterol-pullulan.[32] Till date no reports are available that disclose the potential of poly (ethylene glycol) conjugated gellan polysaccharide micellar carriers in oral controlled drug delivery.

Simvastatin, an anti-hyperlipidemic BCS Class II drug was examined for this novel particulate system because of its poor water solubility (1.3μg/ml at 23°C) and low oral bioavailability due to extensive first pass metabolism in intestinal gut and liver (~5%).[33–35] Furthermore, it showed high variability in pharmacological effects. Thus, the development of an efficient delivery system which could improve oral bioactivity by enhancing its solubility and dissolution rate could be interesting.

GIT offers a wide range of pH and hence, the presence of either weakly acidic or basic functional groups in the polymer chains may cause the polymers to exhibit a pH-dependent behavior. As the absorption of simvastatin occurs mainly in the small intestine, a pH-responsive copolymer could be useful for its delivery to the desired site of action. They can swell or shrink in a controllable manner from changes in the porosity of the polymer network due to pH fluctuations. Thus, polymeric micelles can be developed for preferential release of the encapsulated drug in the intestinal tract, where the uptake of the drug is more likely.[36]

The objective of this work was to modify gellan polysaccharide by conjugating poly (ethylene glycol) chain to its backbone *via* etherification reaction. Confirmation of chemical changes occurred in the copolymer was done by Fourier transform infrared spectroscopy (FTIR), degree of etherification and grafting level. The amphiphilic character and micelle-forming abilities of the copolymer were evaluated. The nanoparticles were further characterized for their size, drug entrapment efficiency, *in vitro* drug release properties and lipid-lowering potentials in rabbit models.

MATERIALS AND METHODS

Materials

Simvastatin was a gift from Mylan Laboratories, Hyderabad, India. Gelrite Gellan gum and dialysis bag (MWCO 3500) were purchased from HiMedia Pvt. Ltd., Mumbai, India. *N, N*-dimethyl formamide (DMF) and PEG 4000 were obtained from Merck Specialities Pvt. Ltd., Mumbai, India. Sodium hydride (60% w/w dispersion in mineral oil) and thionyl chloride were obtained from Spectrochem Pvt. Ltd., Mumbai, India. Pyrene was purchased from Sigma-Aldrich Pvt. Ltd., USA. Cholesterol was procured from Loba Chemie Pvt. Ltd., Mumbai, India. All other reagents were of analytical grade and used as received.

Chlorination of PEG 4000

A solution of 1.5×10^{-5} (M) PEG 4000 in chloroform-thionyl chloride mixture (60 : 40, v/v) was refluxed at room temperature for 3h for chlorination. The reactant mixture was then subjected to heating at 55°C for 30 min to evaporate chloroform. Ten milliliters of water was added and magnetically stirred for 30 min to allow evaporation of gaseous byproducts (SO_2, HCl) generated therein. The product was then cool centrifuged at 8000×g for 30 min at room temperature (C-24 BL, Remi Instruments Ltd., Mumbai, India). The yellowish precipitate was collected and weighed. The supernatant was analysed for estimating the amount of free PEG 4000 by colorimetric assay. One milliliter of supernatant was diluted up to 10ml and 15μl of iodine solution (10mg/ml of iodine and 20mg/ml of potassium iodide) was added.[37] The absorbance of the complex was noted at 540nm using colorimeter (Labard Instrument Pvt. Ltd., LI-129, Kolkata, India). The calculation was made using the slope of a standard curve of PEG 4000 prepared under the same conditions (2–10 μg/ml). Liner regression equation for the standard curve is as follows: $y = 0.053x$, $r^2 = 0.998$. Yield of the chlorinated product was found to be 93.92% and percentage of non-reacted PEG 4000 was found to be 0.077%.

Synthesis of PEG-g-gellan Copolymer

Gellan gum dispersion (6%, w/v) was prepared in DMF and cooled to 10°C. One gram of sodium hydride (NaH) was added to the dispersion and mixed well for 20min. To this, 5.33% (w/v) chlorinated PEG in DMF was added under continuous agitation with a glass rod for 20 min. Total reaction mixture was poured into 50ml of water to remove the excess NaH. The copolymer thus formed was carefully isolated by filtration using muslin cloth and washed with methanol (20ml×3). During the last washing, pH of the copolymer dispersion was adjusted to neutrality with 0.1*N* glacial acetic acid, filtered off, and oven-dried at 40°C. The yield of copolymer sample was found to be 89.63%.

Characterization of the Copolymer

Fourier Transform Infrared Spectroscopy. Potassium bromide (KBr) pellets of PEG 4000, chlorinated PEG 4000, native gellan and the copolymer were made at 125kg/cm^2 hydraulic pressure (KP, Kimaya Engineers, India). These were scanned from 4000 to 400cm^{-1} with a Perkin-Elmer IR Spectrometer (Spectrum RX1, USA) and the spectra were recorded.

Determination of Degree of Substitution. Carbon, hydrogen, and nitrogen content of gellan gum, and copolymer samples were estimated by CHNS/O analyzer (2400 series II, Perkin-Elmer, USA) according to the standard combustion procedure.

The degree of substitution (DS) (fraction of hydroxyl groups modified per average of repeating unit) of PEG moiety onto the copolymer was calculated on basis of carbon content obtained from elemental analysis. Considering that each repeating unit

has 10 hydroxyl groups, the maximum possible DS value would be 10 (100%).[38]

Determination of Grafting Level. The percentage of grafting and grafting efficiency was determined by using the following formulas.[39]

$$\%\ \text{Grafting} = \frac{(\text{weight of grafted product} - \text{weight of native gellan})}{\text{weight of native gellan}} \times 100 \quad (1)$$

$$\text{Grafting efficiency} = \frac{(\text{weight of grafted product} - \text{weight of native gellan})}{(\text{weight of grafted product and residues at the bootm} - \text{weight of native gellan})} \times 100 \quad (2)$$

Determination of CAC. Critical association concentration (CAC) was determined by pyrene fluorescence spectroscopy.[40] Steady-state fluorescence excitation spectra (λ_{em}=390 nm) of pyrene were measured at various copolymer concentration with fluorescence spectrometer (Perkin Elmer, LS55 Fluorescence Spectrometer, USA). Concentrations of polymer were in the range of 0.1–90 mg/l in deionized water at a constant pyrene concentration (2×10^{-7} M).

CAC value of the copolymer was determined using band intensity ratio obtained at 337 nm and 334 nm. Intensity ratio of I_{337}/I_{334} in pyrene excitation spectra was plotted against logarithm of copolymer concentration (log C) and a sigmoidal curve was obtained. The CAC value was determined for the copolymer solution from the intersection of two straight lines (the horizontal line with an almost constant value of the ratio I_{337}/I_{334} and the vertical line with a steady increase in the ratio value).

Preparation of Copolymer Micelles

Required amount of copolymer was added to 10ml of deionized water and allowed to dissolve by stirring in a magnetic stirrer for 30 min and probe sonicated (FS-500, Frontline Electronics and Machinary Pvt. Ltd., Ahmedabad, India) for an additional period of 30 min. The drug was dissolved in 2ml chloroform in a glass syringe. The drug solution was added drop wise into the copolymer solution, which was under continuous magnetic agitation. The stirring was continued up to 4h. Thereafter, the micellar dispersion was filtered by Whatman filter paper no. 1 (pore size 11μm) to remove excess insoluble drug and the filtrate was used for further investigation. Various drug-copolymer weight ratios (1 : 4, 1 : 6, 1 : 8) were used for the preparation of micellar formulations and were designated as F1, F2 and F3, respectively. The drug-free copolymer micelles (F0) were prepared in similar manner.

Characterization of PEG-g-gellan Copolymer Micelles

Microscopic Observation of Micelles. The drug-loaded and drug-free micelles were examined under Magnus digital microscope (Magnus MLX, Olympus, India) at 100× magnification. The photographs were captured by 1.3 mega pixel Moticam 1000 camera using Motic Images Plus 2.0 software (Motic, Canada).

Micellar Size and Zeta Potential. The size and zeta potential of the micellar dispersions were measured by dynamic light scattering using a Malvern Zetasizer Nano ZS90 apparatus (Malvern Instruments, Worcestershire, UK) equipped with a DTS 1060 cell. For the measurement of zeta potential, nanoparticles were suspended in 1 mM NaCl solution. All experiments were performed at 25°C and at measuring angle of 90° to the incident beam.

Estimation of Drug Entrapment Efficiency. Each of the formulations was centrifuged at 8000×g for 30 min (C-24 BL, Remi Instruments Ltd., Mumbai, India). The precipitate was collected, dried at room temperature, weighed and the drug concentration in the micellar phase (D_m) was estimated. Five milliliters of methanol was added to the precipitate and diluted to 10ml with phosphate buffer solution (pH6.8) and the absorbance was measured in UV spectrophotometer (UV1, Thermo Scientific, UK) at 238nm. The drug content in micellar phase (D_m) was estimated by using the slope of the standard curve. From the estimates of drug content, the drug entrapment efficiency was calculated as follows:

$$\text{Entrapment efficiency (\%)} = \frac{\text{actual drug content in the precipitate}}{\text{theoretical drug content in the precipitate}} \times 100 \quad (3)$$

Partition Coefficient and Thermodynamics of Solubilization. After centrifugation of the formulations, the supernatant was analyzed for measuring drug concentration in water (D_w) at 238nm without further dilution. The micelle-water partition coefficient of drug (K) was determined from the following expression:

$$K = \frac{D_m}{D_w} \quad (4)$$

where D_m and D_w are the drug concentration in micellar phase and in water, respectively.

Standard free energy of solubilization (energy required for partitioning of simvastatin from the aqueous phase to the micellar phase) was estimated by the following equation:[41]

$$\Delta G^0 = -RT[\ln K] \quad (5)$$

where R and T represent the universal gas constant and absolute temperature, respectively.

Testing of *In Vitro* Drug Release. The drug release from the micellar formulations were studied with little modification of the conventional *in vitro* dissolution method. Each micellar precipitate was dispersed in 5ml of water and then placed in a dialysis bag and immersed into 200ml of pH6.8 phosphate buffer solution. The dissolution medium was magnetically stirred at 500 rpm (1MLH, Remi Instruments Ltd., Mumbai, India) and was maintained at 37±0.5°C. An aliquot of 2ml was withdrawn from the dissolution medium at specified time intervals and replenished immediately with the same volume of fresh buffer solution. The samples were analyzed spectrophotometrically (UV1, Thermo Scientific, UK) at 238 nm after suitable dilution. Same experimental conditions were followed for carrying out dissolution study in pH1.2 HCl solution. Cumulative percentage of

drug released in the respective dissolution medium was plotted as a function of time. Each study was carried out in triplicate.

Equilibrium Swelling of Copolymer. Swelling property of the copolymer was evaluated in both pH6.8 phosphate buffer and pH1.2 HCl solution. Pre-weighed copolymer samples (100mg) were placed in centrifuge tubes and 5ml buffer was added to each tube. The sample tubes were kept overnight to allow for equilibrium swelling of the copolymer. Thereafter, the sample tubes were subjected to a centrifugal force of 8000×g for 15 min (C-24 BL, Remi Instruments Ltd., Mumbai, India). The supernatant was decanted; the hydrated precipitate was blotted with a tissue paper to absorb surface moisture and weighed. Swelling index was calculated by the following equation:

$$\text{Swelling index}\,(\%) = \frac{W_1 - W_0}{W_0} \times 100 \qquad (6)$$

W_0 indicated initial weight of the copolymer and W_1 was that of the swollen copolymer.

Modeling of Drug Release Data. The mechanism of drug release from the micellar carriers was dictated by the value of diffusion exponent (n) obtained after fitting the drug release data into Korsmeyer–Peppas model: $M_t/M_\infty = kt^n$, where M_t/M_∞ is the fractional solute release at time t and k is a constant that incorporates the structural and geometric characteristics of the device. Liner regression analysis of the plot (logarithm of percentage drug release vs. logarithm of time) was done to evaluate the value for diffusion exponent (n). The drug release mechanism from spherical particles is Fickian mechanism was assumed when n=0.43 or less. Anomalous (non-Fickian) transport mechanism was approximated when the value of n lies between 0.43 and 0.85.[42,43]

Study for Chemical Interference. KBr pellets of pure drug, physical mixture of drug and copolymer (1 : 1) and drug-loaded copolymer carriers were made and the spectra were recorded in Perkin-Elmer FTIR Spectrometer (Spectrum RX1, USA) from 4000 to 400cm^{-1}. Any change in infrared spectrum of the drug was compared with different samples to ascertain drug–polymer interaction.

X-ray Diffraction Study. Pure drug, copolymer and drug-loaded copolymer micelles were scanned from 10–30° 2θ, with X-ray diffractometer (Ultima III, D/Max 2200, Rigaku Corporation., Japan). Cu-Kα radiation; voltage: 40 kV; current: 30mA; scan speed: 5°/min were used to obtain the traces of diffractograms.

Pharmacodynamics on Rabbit Model. This study was approved by Institutional Animal Ethical Committee, Gupta College of Technological Sciences, Asansol (Registration No. 955/RO/a/2006/CPCSEA) *vide* approval no. GCTS/IAEC/2013-Sep/01 dated 10th September, 2013. Male rabbits (1.2-1.5 kg) were housed in a stainless cage and exposed to 12 h light/dark cycle (23±2°C and 40–60% relative humidity). At the end of one week, six rabbits were fed with the regular rabbit diet serving as normal diet controls. Hyperlipidemic rabbits were prepared by feeding HFHC diet for one month. Thereafter, the blood lipid levels were measured. The samples at zero hour were also tested. Hyperlipidemic rabbits were divided into three groups, each consisted of six rabbits. Group I served as control and was treated with physiological saline by gavage. Group II was given an oral treatment with 2.5mg simvastatin suspension/kg body weight per day and that of Group-III with micellar formulation (F3) containing equivalent amount of simvastatin.[44,45] The blood samples were collected from marginal ear vein of the rabbits at 0, 2, 4 and 6h; and serum was separated. Serum samples were analyzed for total cholesterol (TC), low and high density lipoproteins (LDL and HDL), triglycerides and very low density lipoprotein (VLDL) by *in vitro* diagnostic kits (Span Diagnostics Ltd., Surat, India).

Data Analysis

The difference in drug entrapment efficiency of the formulations was analyzed by one-way analysis of variance (ANOVA). Statistical differences in lipid profiles of treatment and control groups were done by one-way analysis of variance (ANOVA) followed by Dunnets post test ($n = 6$) using GraphPad Prism software (Version 3.00). $P<0.05$ was set as a criterion for significant difference.

RESULTS AND DISCUSSION

Synthesis and Characterization of Copolymer

Unmodified gellan gum possesses –OH functional groups which are amenable to various chemical modifications including etherification. The synthesis of copolymer involved the following steps: (i) chlorination of PEG 4000; (ii) formation of gellan alkoxide; and (iii) reaction between chlorinated PEG and gellan alkoxide for the formation of covalent ethereal linkage.

The chlorination of PEG 4000 and the formation ether linkage were confirmed by infrared analysis. In the FTIR spectrum of PEG 4000, O-H stretching frequency was noted at 3422.39 cm^{-1}. C-O-C stretching and C-H stretching frequency was observed at 1107.00 cm^{-1} and 2897.67 cm^{-1} [Figure 1(a)].[46,47] These characteristics peaks shifted to lower wave numbers at 1105.31 cm^{-1} and 2862.74 cm^{-1}, respectively in the spectrum of chlorinated PEG [Figure 1(b)]. The appearance of a new peak at 674.15 cm^{-1} was assigned to C-Cl stretching of chlorinated PEG.[48] O-H stretching peak was almost absent in

$$\text{PEG 4000} + SOCl_2 = Cl-(CH_2CH_2O)_n-CH_2CH_2Cl + SO_2\uparrow + HCl\uparrow$$

$$\text{Gellan}-OH + NaH = \text{Gellan}-ONa + 2H_2$$

$$[\text{Glucose}-CH_2ONa(\beta1\rightarrow4)D-\text{Glucuronic acid}(\beta1\rightarrow4)D$$

$$-\text{Glucose}-CH_2ONa\,(\beta1\rightarrow4)$$

$$\text{L}-\text{Rhamnose}\,(\alpha1\rightarrow3)]n + Cl-(CH_2CH_2O)_n-CH_2CH_2Cl$$

$$= [\text{Glucose}-\text{Glucuronic acid}-\text{Glucose}-\text{Rhamnose})]n + 2NaCl$$

$$(6)CH_2O-(CH_2CH_2O)_nCH_2CH_2Cl$$

the spectrum of chlorinated PEG. This confirmed end-capped chlorination of the PEG chain on both sides [Figure 1(b)].

FTIR spectroscopy of Gelrite gellan showed characteristics stretching of hydrogen-bonded OH groups of glucopyranose moiety at 3364.64 cm^{-1} in Figure 1(c). An intense peak at 2924.82 cm^{-1} indicated the stretching of -CH and -CH$_2$ groups.[13] Carboxyl stretching was noted at 1415.38 cm^{-1}.[49] This band shifted slightly to 1466.50 cm^{-1} in the copolymer [Figure 1(d)]. In FTIR spectrum of the copolymer, a new sharp band was noted at 1114.75 cm^{-1} and this was attributed to C-O-C stretching of alkyl ether [Figure 1(d)]. This confirmed etherification reaction between gellan polysaccharide and PEG

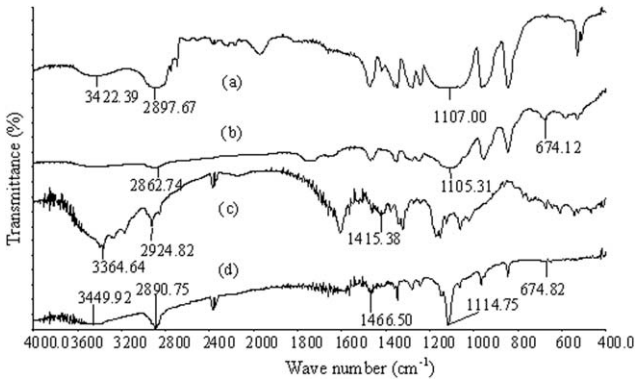

Figure 1. FTIR spectra of (a) PEG 4000; (b) PEG-Cl; (c) Gelrite gum and (d) Copolymer.

chain. It was interesting to note that a weak peak of C-Cl stretching was also observed in the spectrum of copolymer at 674.82 cm^{-1}, thus excluding the possibility of conjugation of both ends of PEG to the gellan polysaccharide backbone.

CHN analysis of the native gellan and copolymer samples further confirmed the grafting reaction. In native gellan, the content of C, H, and N was 37.44%, 5.89% and 0.22%, respectively. A trace of nitrogen was attributed to the presence of protein impurities in the gum. The same was found to be in the order of 54.26%, 9.03% and 0.02%, respectively. It was evident that the percentage of carbon and hydrogen in the copolymer was relatively higher than native gellan. This was possible only when PEG was grafted successfully onto gellan gum backbone. Percentage of grafting and the efficiency of grafting were found to be 34.44% and 74.69%, respectively. The degree of PEG substitution was low (5.99%) in the copolymer (Table I). Gelrite possess 10 hydroxyl groups per repeating unit and hence, a degree of substitution would reach 100% if all hydroxyl groups are substituted. Earlier it was established that at alkaline condition, the hydroxyl groups at C-6 position was the most reactive functional groups because the vicinal hydroxyl groups had a tendency to form relatively strong adducts rather than the generation of oxyanions.[50] Therefore, it was assumed that at least one hydroxyl group per two repeating units of Gelrite was substituted with PEG under the conditions specified in the synthetic procedure.

Properties of Micelles

Microscopic observations of aqueous copolymer dispersion revealed the spherical structures of copolymer micelles [Figure 2(a)]. At the beginning, some trials were set to examine amphiphilic nature of the copolymer. PEG-gellan copolymer was dissolved in water and the solution was observed under microscope. Out of them, some of these samples were found to form micellar structures. The formation of micellar structures by the copolymer can be explained as follows. PEG block is generally treated as hydrophilic moiety. An earlier study demonstrated that PEG could serve as hydrophobic block of PEG-*b*-polyvinyl alcohol copolymer after addition of sodium chloride.[51] The investigators stated that the solubility of PEG in aqueous solution deteriorated after addition of salts and the copolymer exhibited its amphiphilic property in aqueous solution. In this work, both ends of PEG were capped with chlorine (Cl) groups to reduce its hydrophilicity. Because one of them reacted with gellan alkoxide for establishing covalent ether linkage, the other remained free and single end-capped chlorinated PEG served its hydrophobic role in the amphiphilic copolymer.

In order to have an understanding of the onset of micellization, the CAC value of copolymer was determined by pyrene fluorescence spectroscopy. A graph with two linear segments having different slopes was represented in Figure 3. The intersection point of these two segments was recognized as CAC value and was 9.12 mg/l in water for the copolymer under investigation. A lower CAC value of the copolymer was evident from the graph. Before fluorescence spectroscopy, the hydrophobic pyrene probe was added to copolymer solutions of increasing concentration, and pyrene excitation spectra were recorded for all solutions. At low copolymer concentration, low pyrene intensity was observed because it sensed a polar aqueous environment but beyond a specific copolymer concentration, pyrene intensity increased due to preferential partitioning of the probe into hydrophobic core of micelles.[52,53]Pyrene is hydrophobic and sensed hydrophobic environment to a considerable extent as the micellar structures were formed. This property of pyrene was utilized for the determination of CAC value. Above a certain copolymer concentration, the intensity gradually increased with higher copolymer concentration and was thought of as the onset of micellization.

The drug-loading into copolymer micelles was accomplished by solvent evaporation method as a function of drug: copolymer weight ratio (1 : 4 to 1 : 8, w/w). The drug-loaded micelles appeared spherical when observed under microscope and no morphological difference was realized. A representative photograph was displayed in Figure 2(b). By setting the drug concentration at a constant level, the variation in drug: copolymer ratio caused a significant deviation ($p<0.05$) in mean drug entrapment efficiency of the micellar formulations. A maximum of 18.86% drug entrapment efficiency was envisaged at the

Table I. Determination of Degree of Substitution of PEG Chain by Elemental Analysis

	Average carbon percentage	Mole number	Degree of substitution (per repeating subunit)
Gellan gum (24 carbon/molecule)	37.44[a]	37.44/(24×12)= 0.13	
PEG-gellan copolymer	54.26[a]	-	5.99%
PEG 4000 (180 carbon/molecule)	16.82[b]	16.82/(180×12)= 0.0078	

[a] From CHN analysis; Difference between gellan gum and PEG-grafted-gellan copolymer.

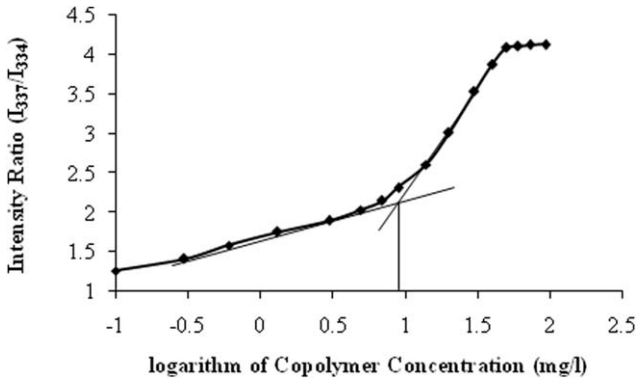

Figure 2. Plot of intensity ratio (I_{337}/I_{334}) from pyrene excitation spectra versus logarithm of copolymer concentration (C) in distilled water.

highest ratio (Table II). This was explained by Gibb's free energy change. The copolymer micellar systems had comparatively higher micelle-water partition coefficient values than gellan-PEG mixture and thus, the negative free energy of solubilization was found higher for the copolymer (Table II). Moreover, the negative free energy of solubilization gradually increased with increasing copolymer concentration. Hence, it was said that the copolymer favored self-aggregation at higher copolymer concentration and entrapped higher amount of drug into micellar structures (Table II).[54]

The drug entrapment efficiency of gellan-PEG micelles increased with increasing drug: copolymer ratio. For a fixed pay load of 15% (w/w), a maximum of 4.0 and 4.8% (w/w) cyclosporine A entrapped into dextran-PEG-C_{16} (3 mol %) and dextran-PEG-C_{16} (7 mol %) copolymer micelles, respectively.[55] The drug entrapment efficiency of the newly developed copolymer micelles was about 4 times higher than dextran-PEG micelles. Thus, it was thought that the micropolarity of PEG-Cl core was slightly better than dextran-PEG-C_{16} core. However, further work is necessary for the improvement of drug entrapment efficiency of the micelles.

The drug-loaded micelles had diameters in between 426.8 and 912.6 nm with a polydispersity index <0.761 and their size dropped with higher drug load (Table II). Presumably, the encapsulation of drug enhanced the hydrophobic interactions in the core and produced more compact particles.[56] The size of PEG-gellan copolymer micelles was larger than that of other polysaccharide-based micelles available in the art. Probably, gellan polysaccharide and PEG chains induced larger steric hindrances over a larger volume for the polymer of higher molecular weight[57,58] and thus led to the formation of larger particle size. The aqueous copolymer dispersion was physically stable due to their high negative zeta potential values (−26.3 to −28.4 mV) (Table II). On physical verification, no sign of aggregation was evident even after three months' monitoring of the preparations. The drug-free micelles showed a zeta potential value of −28.0 mV. No appreciable difference in the zeta potential values of unloaded and drug-loaded micelles was envisaged as a consequence of simvastatin loading into the micelles. The degree of electrostatic repulsion between adjacent, negatively charged particles in dispersion was higher for both unloaded and drug-loaded micelles [59] and afforded physical stability to the micellar dispersion.

Water is a non-selective solvent for both PEG and gellan gum. To have an understanding of relative hydrophobic property of these polymers, zeta potential value for the drug-free copolymer dispersion was measured (−28.0 mV). Gellan gum is an anionic polymer due to presence of negatively charged carboxyl groups in its structure and thus may exhibit negative zeta potential. Indeed, it was not hard to say that gellan gum acted as a hydrophilic shell for the copolymer. This was further confirmed by the fact that the copolymer particles precipitated out from its aqueous dispersion with the addition of divalent calcium ions. Water readily forms hydrogen bonds with the polar groups such as OH present in PEG 4000 but chlorination on both ends resisted such interaction and consequently, lowered its hydrophilicity. The adsorption property of PEG, capped at one end with fluorocarbon groups was reported by Richards and coworkers.[60] They concluded that the adsorption of PEG at the air–water interface became higher as the hydrophobic fluorocarbon group was inserted at one end of PEG. Lastly, it was understood that the relatively hydrophobic PEG chains of copolymer created a core and the gellan polysaccharide chains formed the hydrophilic corona and assumed micellar structures in water. In brief, two segments of the copolymer arranged themselves in accordance with the polarity of dispersion medium.

Swelling and Drug Release Potential

In vitro drug release profiles of the copolymer nanoparticles were dictated in Figure 4. It was obvious that the drug release rate was significantly higher in phosphate buffer solution than in HCl solution. Only 14–16% drug was found to release in acidic medium. On contrary, the same was about 36–44% in 2h in phosphate buffer solution. Swelling index was found to be 20.2% and 28.9% for pH1.2 HCl solution and pH6.8 phosphate buffer solution, respectively. An initial burst release of drug (26–35%) was noticed in pH6.8 phosphate buffer solution from all of the formulations at the first hour. The sudden release of drug molecules adsorbed or weakly held onto the hydrophilic surface of the copolymer micellar structures could be responsible for such burst effect. Because gastrointestinal tract exhibits a wide pH range, the copolymer was said to exhibit pH-dependent

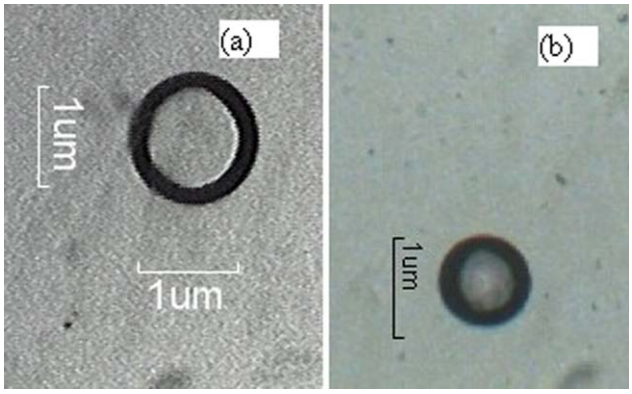

Figure 3. Microscopic images of (a) drug-free copolymer micelles and (b) drug-loaded micellles at 100× magnification. [Color figure can be viewed in the online issue, which is available at wileyonlinelibrary.com.]

Table II. Effect of Drug Loading on Drug Entrapment Efficiency, Mean Diameter, Zeta Potential Values and Thermodynamics of Micellar Solubilization

Formulation	Entrapment efficiency (%) (Mean ± SD, $n=3$)	Mean diameter (nm)	Zeta potential (mV)	Partition coefficient (K)	ΔG^O (KJ/mole)
F0	-	706.3	−28.0	-	-
F1	10.47± 0.72	612.6	−27.4	36.14	−9.245
F2	14.79±1.08	526.6	−28.4	57.07	−10.423
F3	18.86±0.88	426.8	−26.3	77.83	−11.223
PM[a]	-	-	-	1.19	-0.448

[a] Physical mixture of gellan gum and PEG 4000 (1 : 1) in water

behavior. The swelling and shrinking propensities of the particles were associated with changes in porosity of the copolymer network due to pH fluctuations. Hence, the copolymer micelles favored the release of encapsulated drug in the pH prevailing in small intestinal region. Carboxyl groups of gellan gum remained unionized in acidic media, swelled less and ensued release of a small amount of drug. This phenomenon was quite opposite in alkaline media. Due to repulsion of negatively charged carboxyl groups, the copolymer micelles perhaps swelled more and released more amount of drug in alkaline media.

To explain the drug release mechanism, the drug release data obtained up to 60% in pH6.8 phosphate buffer solution was fitted into the Korsmeyer-Peppas equation. Irrespective of drug: copolymer ratio, the values of n ranged between 0.514 and 0.668 with good correlation coefficients (r^2) of 0.966-0.988 (Table III). Hence, the drug transport from the micellar formulations was said to follow anomalous (non-Fickian) diffusion mechanism, *i.e.* the drug release was controlled by a combination of simple diffusion and polymer relaxation. In order to find out the relative contribution of these two processes, the drug release data was further fitted into Peppas-Sahlin equation:[61]

$$\frac{M_t}{M_\infty} = k_1 t^m + k_2 t^{2m} \quad (7)$$

where the first term of the right hand side was the Fickian contribution, the second term being the Case-II relaxational contribution. The coefficient m was the purely Fickian diffusion exponent for a device of any geometrical shape. Usually, the value of m was 0.43 for any spherical devices. Non-linear regression analysis of equation (7) solved the values of k_1 and k_2 (Table II). It was observed that $k_1 >> k_2$ and this was suggestive of significant contribution of Fickian diffusion over copolymer relaxation.

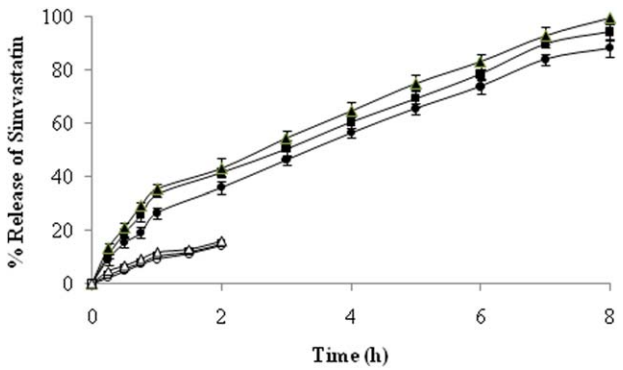

Figure 4. Drug Release profiles of copolymer nanoparticles in pH1.2 HCl and pH 6.8 phosphate buffer solution. Key: (•) F1; (■) F2 and (▲) F3 (phosphate buffer solution) and (○) F1; (□) F2 and (Δ) F3 (HCl solution). [Color figure can be viewed in the online issue, which is available at wileyonlinelibrary.com.]

Physicochemical Compatibility

In the spectrum of pure drug [Figure 5(a)], free O-H stretching of OH group was noted at 3552.08 cm^{-1}. Carbonyl stretching (C=O) vibration was found at 1725.87 cm^{-1} and 1700.69 cm^{-1} due to lactone and ester C=O groups, respectively.[62] The peaks at 1165.89 cm^{-1} and 1055.47 cm^{-1} were ascribed to C-O-C bending vibration of lactone and ester functional groups.[45] In the spectrum of physical mixture, all characteristic peaks of the drug were retained [Figure 5(b)]. In FTIR spectrum of micellar formulation, free O-H stretching peak of pure drug shifted to 3449.92 cm^{-1}. A weak intermolecular hydrogen bonding between OH^- groups of drug and copolymer may exhibit this kind of behavior. However, a change of about 2 cm^{-1} in wave number could be considered insignificant. The presence of characteristics infrared peaks of pure drug persisted in the spectrum of the drug-loaded micelles and hence, the evidence of drug-copolymer interaction was not impreesive.

X-ray diffraction pattern of pure drug exhibited sharp peaks of higher intensity at the diffraction angles of 10.86°, 11.70°, 16.18°, 18.74-19.02°, 19.30-19.46°, 20.68-21.04°, 21.8–21.88°, 22.74-22.88°, 23.00–23.20°, 27.60-27.68° and 30.14–30.24°2θ. This was characteristics of crystalline form of the drug. Similar

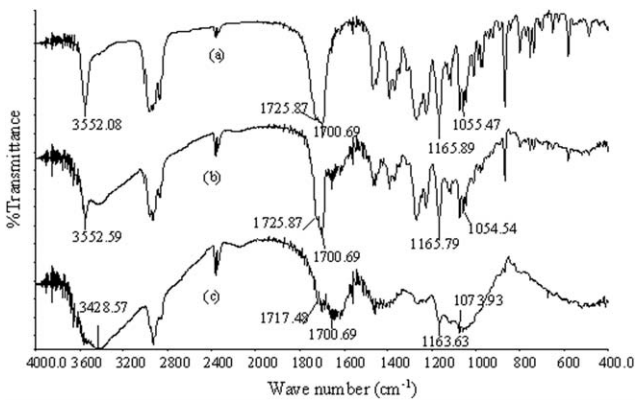

Figure 5. FTIR spectra of (a) pure drug, (b) physical mixture and (c) micellar formulation.

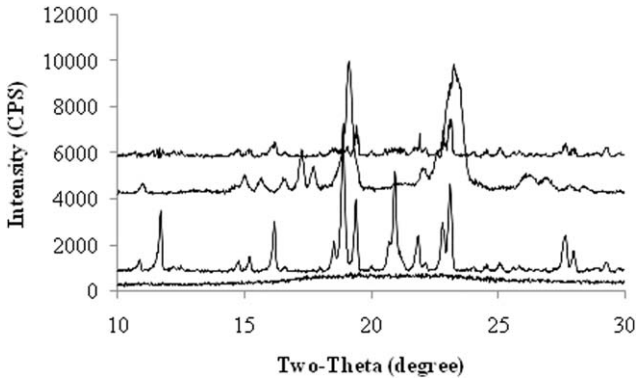

Figure 6. X-ray diffraction pattern of (a) copolymer; (b) pure drug; (c) physical mixture; and (d) micellar formulation.

peaks were identified at these diffraction angles for the sample of physical mixture. No such intense peaks were noted for the copolymer (Figure 6). The characteristics peak intensity of pure drug reduced to an appreciable extent in the diffractogram of drug-loaded micelles. The reduction of crystallographic peak intensities provided an indication of polymorphic transition following entrapment of drug into copolymer micelles. This observation was quite similar to that reported by Choi *et al.*[63] and Li *et al.*[64]

Effect on Lipid Profiles

Serum lipid profiles of experimental rabbits following oral administration of micellar formulations and pure drug dispersion were demonstrated in Table IV. In hyperlipidemia, one or more of the plasma lipids are usually elevated, in which statins offer an effective means of treatment. Simvastatin (HMG-CoA reductase inhibitor) reduces the elevated total cholesterol, triglycerides, LDL-cholesterol and VLDL-cholesterol levels in hyperlipidemic conditions. At the same time, it causes the elevation of HDL-cholesterol levels, which promote the removal of cholesterol from peripheral cells and facilitate its delivery back to the liver.[65] This effect was dose-dependent and hence, could be used as a basis for comparison of *in vivo* performance of pure drug and the formulation.

It was observed that the dispersion of pure drug decreased total cholesterol level by 13.31%, TG by 18.12%, LDL cholesterol by 19.03%, and increased HDL cholesterol by 11.86% at the end of 6h following oral administration. On contrary, the micellar formulation reduced total cholesterol level by 30.15%, TG by 20.66%, LDL cholesterol by 44.63%, and increased HDL cholesterol by 21.38% after 6h of administration. Thus, micellar formulation performed better than pure drug in reducing total cholesterol, LDL and TG levels. This could primarily be attributed to the improved solubility and dissolution rate of the drug associated with its polymorphic transformation to amorphous state.[66] Similar observation was reported by Rao *et al.*[44] and Singh *et al.*[45]

A comparison among groups by ANOVA revealed a statistically significant difference ($p<0.05$). Dunnets post test compared the control group with the reference and test groups. Except for the serum HDL cholesterol profiles, the comparison of other lipid profiles of test and reference groups with respect to control demonstrated significant differences ($p<0.05$). With respect to HDL profile, no significant difference persisted between control and reference groups ($p<0.05$) but that did between control and test groups ($p>0.05$). The lipid-lowering potential of the copolymer micelles was encouraging. A recent report indicated that the patients with elevated LDL-C, low HDL-C, and elevated triglycerides had increased risk for coronary heart disease (CHD). Likewise, simvastatin therapy could be beneficial.[67] In view of this; the newly designed micellar carrier could be an effective drug delivery system which would minimize the incidence of CHD. Further, negatively charged particles are known to possess bioadhesive properties which can favor the drug absorption *via* transcytosis pathway from intestine and accumulate in the blood stream. Due to their small size, the nanoparticles may further be localized at the M-cells of Peyer's patches and easily transcytosed[28,68] and consequently improve pharmacodynamic activity of the micellar preparations.

In continuation with our earlier discussion, the authors would like to emphasize on the possibility of clinical studies of the newly developed polymeric micelles in relation to the current regulatory environment. Nanomedicines which do not require the use of toxic solvents or do require minimal use of solvents offer clear advantages over their conventional counterparts. It is well understood that subtle changes in composition arising from small deviations in the manufacturing process could result in substantial changes in pharmacology and toxicity of nanomedicines. Usually, the manufacture of nanoparticles often requires multiple process steps involving multi-component systems. Current nanosystems do not involve multiple steps, thus allowing easy scale-up and manufacturing.

The FDA highlighted the importance and challenges in maintaining a close control over the manufacturing process in draft guidance for liposome drug products stating that "liposome drug products are sensitive to changes in the manufacturing conditions like scale, shear force, and temperature. The present approach circumvents the complex manufacturing steps of creating a stable finished nanomedicine and may significantly reduce the cost of manufacturing and forego the complex development work it

Table III. Mathematical Modeling of Drug Release Data Obtained at pH6.8 Phosphate Buffer Solution

	Korsmeyer-Peppas Model			Peppas-Sahlin Model		
Formulation Code	n	k	r^2	k_1	k_2	r^2
F1	0.668	0.2409	0.988	0.150	0.089	0.9977
F2	0.588	0.2818	0.966	0.216	0.069	0.9929
F3	0.514	0.3083	0.968	0.247	0.065	0.9952

Table IV. Serum Lipid Profiles of Various Group of Rabbits at Different Time Intervals

Group	Time (hour)	TG (mg/dl)	Total cholesterol (mg/dl)	HDL Cholesterol (mg/dl)	LDL Cholesterol (mg/dl)
Group I (Control)	0	87.0±2.13	160.4±1.01	31.0±1.92	112.0±3.01
	2	89.5±1.72	163.6±2.15	30.2±0.89	115.5±3.06
	4	91.0±2.01	164.4±3.12	32.2±1.12	114.0±2.15
	6	93.0±3.56	168.7±2.69	33.1±2.59	117.0±5.44
Group II (Reference)	0	69.0±1.18	161.5±2.32	29.5±1.75	118.2±1.22
	2	64.0±1.85	158.0±2.65	30.0±1.67	115.2±1.09
	4	63.0±2.02	146.3±2.09	32.3±1.89	101.4±1.93
	6	56.5±0.46	140.0±2.35	33.0±2.09	95.7±2.91
Group III (Test)	0	75.0±1.11	169.8±2.72	31.8±0.63	123.0±1.56
	2	74.0±1.44	149.3±1.93	32.8±0.34	101.7±1.89
	4	64.0±1.38	137.0±2.14	34.5±0.97	89.7±0.97
	6	59.5±1.57	118.6±3.92	38.6±2.04	68.1±2.10

would involve. Unlike liposomes, the use of hydrophilic PEG is no longer required to provide stability and long-circulating characteristics to the core-shell nanoparticulate systems.

In reality, a new nanoparticle-based medicine needs to successfully overcome several hurdles before it is approved for marketing. These include the development of the nanostructure with appropriate components and properties, reproducible manufacturing process, favorable pharmacology and toxicity profile, and demonstration of safety and efficacy in clinical trials. While conceptually these are similar hurdles that may be faced by any new drug, the particular complexity and multi-component nature of nanomedicines introduce large number of additional variables that may substantially increase the level of difficulty in controlling processes and predictability of behavior in a biological system. However, the nanosystems of our present investigation showed immense potential in overcoming the major hurdles like easy scale-up process, non-requirement of additional stabilizer, single step manufacturing process, and safety concerns due to use of non-toxic, biodegradable biopolymer and significant bioactivity in animal models. Although, conventional animal models may be insufficient to correctly extrapolate and predict nanoparticle biodistribution and toxicity in humans, this study simplified the regulatory challenges/complexity of nanomedicine products and opened up the possibility of performing clinical studies in order to access new and innovative treatments.

CONCLUSION

An amphiphilic copolymer was synthesized by grafting PEG chain onto gellan polysaccharide backbone. The copolymer associated in water to form spherical micellar particles and enhanced aqueous solubility of simvastatin by about 66 folds. Nanomicellar particles provided control drug release profiles in phosphate buffer solution. Lower CAC and higher negative zeta potential of the copolymer suggested physical stability of its micellar structures. Further, no appreciable drug-polymer chemical interaction was evident. X-ray analysis suggested a considerable reduction of drug's crystallinity. The lipid lowering action of the particulate system was excellent and comparable. The nanoparticles formed by dual hydrophilic polymers exhibited excellent lipid lowering activity and thus, offered great promise in the delivery of poorly soluble drugs like simvastatin.

ACKNOWLEDGEMENT

The authors express their gratitude to all the management members of Trinity Trust, Asansol, West Bengal for their encouragement and kind co-operation to accomplish this work successfully.

REFERENCES

1. Shah, D. P.; Jani, G. K. *Pharm. Technol.* **2009**, *33*, 48.
2. Kang, K. S.; Veeder, G. T.; Mirrasoul, P. J.; Kaneko, T.; Cottrell, I. W. *Appl. Environ. Microbiol.* **1982**, *43*, 1086.
3. Rozier, A.; Mazuel, C.; Grove, J.; Plazonnet, B. *Int. J. Pharm.* **1997**, *153*, 191.
4. Sanzgiri, Y. D.; Maschi, S.; Crescenzi, V.; Callegaro, L.; Topp, E. M.; Stella, V. J. *J. Control. Release* **1993**, *26*, 195.
5. Kedzierewicz, F.; Lombry, C.; Rios, R.; Hoffman, M.; Maincent, P. *Int. J. Pharm.* **1999**, *178*, 129.
6. Santucci, E.; Alhaique, F.; Carafa, M.; Coviello, T.; Murtas, E.; Riccieri, F. M. *J. Control. Release* **1996**, *42*, 157.
7. Miyazaki, S.; Aoyama, H.; Kawasaki, N.; Kubo, W.; Attwood, D. *J. Control. Release* **1999**, *60*, 287.
8. Agnihotri, S. A.; Jawalkar, S. S.; Aminabhavi, T. M. *Euro. J. Pharm. Biopharm.* **2006**, *63*, 249.
9. Rajnikanth, P. S.; Balasubramaniam, J.; Mishra, B. *Int. J. Pharm.* **2007**, *335*, 114.
10. Patil, J. S.; Kamalapur, M. V.; Marapur, S. C.; Shiralshetti, S. S. *Indian J. Pharm. Sci.* **2011**, *73*, 504.
11. Yang, F.; Xia, S.; Tan, C.; Zhang, X. *Eur. Food Res. Technol.* **2013**, *237*, 467.
12. Emeje, M. O.; Franklin-Ude, P. I.; Ofoefule, S. I. *Int. J. Biol. Macromol.* **2010**, *47*, 158.
13. Shah, D. P.; Jani, G. K. *Ars. Pharm.* **2010**, *51*, 28.
14. Ali, J.; Md, S.; Baboota, S.; Sahni, J. K. In Patenting Nanomedicines: Legal Aspects, Intellectual property and Grant

Opportunity; Souto, E. B., Ed.; Springer-Verlag Berlin Heidelberg: New York, **2012**; Vol. *24*, Chapter 4, pp 103.

15. Rajaonarivony, M.; Vauthier, C.; Couarraze, G.; Puisieux, F.; Couvreur, P. *J. Pharm. Sci.* **1993**, *82*, 912.
16. Sarmento, B.; Ribeiro, A.; Veiga, F.; Neufeld, R.; Ferreira, D. *Revista Portuguesa Farmacia* **2005**, *LII*, 139.
17. Yokoyama, M.; Miyauchi, M.; Yamada, N.; Okano, T.; Sakurai, Y.; Kataoka, K.; Inoue, S. *Cancer Res.* **1990**, *50*, 1693.
18. Torchilin, V. P. *J. Control. Release* **2001**, *73*, 137.
19. Kwon, G. S. *Adv. Drug Deliv. Rev.* **2002**, *54*, 167.
20. Kataoka, K. *J. Macromol. Sci. Pure Appl. Chem.* **1994**, *A31*, 1759.
21. Hofland, H. E.; Bouwstra, J. A.; Verhoef, J. C.; Buckton, G.; Chowdry, B. Z.; Ponec, M.; Junginger, H. E. *J. Pharm. Pharmacol.* **1992**, *44*, 287.
22. Kim, S. C.; Kim, D. W.; Shim, Y. H.; Bang, J. S.; Oh, H. S.; Wan, K. S.; Seo, M. H. *J. Control. Release* **2001**, *72*, 191.
23. Jevprasesphant, R.; Penny, J.; Attwood, D.; McKeown, N. B.; D'Emanuele, A. *Pharm. Res.* **2003**, *20*, 1543.
24. Charman, W. N.; Stella, V. *J. Adv. Drug Deliv. Rev.* **1991**, *7*, 1.
25. Horter, D.; Dressman, J. B. *Adv. Drug Deliv. Rev.* **2001**, *46*, 75.
26. Chen, H.; Langer, R. *Adv. Drug Deliv. Rev.* **1998**, *34*, 339.
27. Torchilin, V. P. *Pharm. Res.* **2007**, *24*, 1.
28. Francis, M. F.; Cristea, M.; Winnik, F. M. *Pure Appl. Chem.* **2004**, *76*, 1321.
29. Francis, M. F.; Cristea, M.; Winnik, F. M. *Biomacromolecules* **2005**, *6*, 2462.
30. Jeong, Y. -Il.; Seo, D. -H.; Kim, D. -G.; Choi, C.; Jang, M. -K.; Nah, J. -W. *Macromol. Res.* **2009**, *17*, 538.
31. Ouchi, T.; Minari, T.; Ohya, Y. *J. Polym. Sci. A. Polym. Chem.* **2004**, *42*, 5482.
32. Akiyoshi, K.; Kobayashi, S.; Shichibe, S.; Mix, D.; Baudys, M.; Kim, S. W.; Sunamoto, J. *J. Control. Release* **1998**, *54*, 313.
33. Kang, B. K.; Lee, J. S.; Chon, S. K.; Jeong, S. Y.; Yuk, S. H.; Khang, G.; Lee, B. H.; Cho, S. H. *Int. J. Pharm.* **2004**, *274*, 65.
34. Ambike, A. A.; Mahadik, K. R.; Paradkar, A. et al. *Pharml. Res.* **2005**, *22*, 990.
35. Shitara, Y.; Sugiyama, Y. *Pharmacol. Ther.* **2006**, *112*, 71.
36. Colombo, P.; Sonvico, F.; Colombo, G.; Bettini, R. *Pharm. Res.* **2009**, *26*, 601.
37. Yoncheva, K.; Doytchinova, I.; Irache, J. M. *Drug Dev. Ind. Pharm.* **2010**, *36*, 676.
38. Ibrahim, N. A.; Yunus, W. M. Z. W.; Abu-Ilaiwi, F. A.; Rahman, M. Z. A.; Ahmad, M. B.; Dahlan, K. Z. M. *J. Appl. Polym. Sci.* **2003**, *89*, 2233.
39. Mendes, A. C.; Baran, E. T.; Nunes, C.; Coimbra, M. A.; Azevedo, H. H. S.; Reis, R. L. *The Royal Society of Chemistry* **2011**, (Supporting Online Material).
40. Bajgai, M. P.; Aryal, S.; Lee, D. R.; Park, S. J.; Kim, H. Y. *Colloid Polym. Sci.* **2008**, *286*, 517.
41. Kulthe, S. S.; Inamdar, N. N.; Choudhari, Y. M.; Shirolikar, S. M.; Borde, L. C.; Mourya, V. K. *Colloids Surf. B Biointerfaces* **2011**, *88*, 691.
42. Korsmeyer, R. W.; Gurny, R.; Doelker, E.; Buri, P.; Peppas, N. A. *Int. J. Pharm.* **1983**, *15*, 25.
43. Ritger, P. I.; Peppas, N. A. *J. Control. Release* **1987**, *5*, 37.
44. Rao, M. Y.; Thanki, K.; Bhise, S. *Dissolution Technol.* **2010**, *17*, 27.
45. Singh, H.; Philipa, B.; Pathak, K. *Iran J. Pharm. Res.* **2012**, *11*, 433.
46. Patil, M. P.; Gaikwad, N.*J. Acta Pharm.* **2009**, *59*, 57.
47. Parmar, K. R.; Shah, S. R.; Sheth, N. R. *Dissolution Technol.* **2011**, *8*, 55.
48. Yue-Jian, C.; Juan, T.; Fei, X.; Jia-Bi, Z.; Ning, G.; Yi-Hua, Z.; Ye, D.; Liang, G. *Drug Dev. Ind. Pharm.* **2010**, *36*, 1235.
49. Jaya Prakash, S.; Santhiagu, A.; Jasemine, S. *J. Pharmceutical BioSciences* **2014**, *2*, 63.
50. Yalpani, M. In Carbohydrates: Structures, Syntheses and Dynamics; Finch, P. (Ed.); Kluwer Academic: Publishers: Germany, **1999**; Vol. *12*, Chapter 8, pp 294–318.
51. Zhou, J.; Ke, F.; Tong, YT.; Li, Z.; Liang, D. *Soft Matter* **2011**, *7*, 9956.
52. Zhao, C. L.; Winnik, M. A.; Riess, G.; Croucher, M. D. *Langmuir* **1990**, *6*, 514.
53. Dong, D. C.; Winnik, M. A. *Can. J. Chem.* **1984**, *62*, 2560.
54. Shi, B.; Fang, C.; You, M.; Zhang, Y.; Fu, S.; Pei, Y. *Colloid Polym. Sci.* **2005**, *283*, 954.
55. Francis, M. F.; Lavoie, L.; Winnik, F. M.; Leroux, J.-C. *Euro. J. Pharm. Biopharm.* **2003**, *56*, 337.
56. Zhang, N.; Wardwell, P. R.; Bader, R. A. *Pharmaceutics* **2013**, *5*, 329.
57. Baldwin, A. L.; Chien, S. *Arteriosclerosis* **1988**, *8*, 140.
58. Maksimenko, A. V.; Schechilina, Y. V.; Tischenko, E. G. *Biochemistry (Mosc)* **2001**, *66*, 456.
59. Hanaor, D. A. H.; Michelazzi, M.; Leonelli, C.; Sorrell, C. C. *J. Euro. Ceramic Soc.* **2012**, *32*, 235.
60. Richards, R. W.; Sarica, J.; Webster, J. R. P.; Holt, S. A. *Langmuir* **2003**, *19*, 7768.
61. Peppas, N. A.; Sahlin, J. *J. Int. J. Pharm.* **1989**, *57*, 169.
62. Mandal, D.; Ojha, P. K.; Nandy, B. C.; Ghosh, L. K. *Der Pharmacia Lettre* **2010**, *2*, 47.
63. Choi, K. C.; Bang, J. Y.; Kim, P. I.; Kim, C.; Song, C. E. *Int. J. Pharm.* **2008**, *355*, 224.
64. Li, X.; Zhang, Z.; Li, J.; Sun, S.; Weng, Y.; Chen, H. *Nanoscale* **2012**, *4*, 4667.
65. Rajyalakshmi, G.; Reddy, A. R. N.; Rajesham, V. V. *Int. J. Pharmacol.* **2008**, *6*, 10.
66. Paradkar, A.; Anshuman, A.; Mahadik, K. R. *Pharm. Res.* **2005**, *22*, 990.
67. Ballantyne, C. M.; Olsson, A. G.; Cook, T. J.; Mercuri, M. F.; Pedersen, T. R.; Kjekshus, J. *Circulation* **2001**, *104*, 3046.
68. Hongming, C.; Robert, L. *Adv. Drug Deliv. Rev.* **1998**, *34*, 339.